Monte Carlo studies of the dynamic behavior of the reduction reaction of NO by CO over a surface of clusters supported on a fractal

Joaquín Cortés* and Eliana Valencia
Facultad de Ciencias Físicas y Matemáticas, Universidad de Chile, Casilla 2777, Santiago, Chile
(Received 30 August 2004; published 22 April 2005)

A Monte Carlo simulation study is made of the dynamic behavior of the reduction reaction of NO by CO, assuming an experimentally representative mechanism, over a catalytic substrate consisting of clusters of active sites supported on a fractal. Various empirical laws are found for the evolution in time of production over various cyclic graphs or trees that represent the various clusters of catalytic sites on the surface. An analysis is made of the phase diagrams and the production achieved versus concentration of the gas phase at different temperatures.

DOI: 10.1103/PhysRevE.71.046136 PACS number(s): 05.70.−a

I. INTRODUCTION

Surface reactions under flow conditions are good examples of irreversible dynamic systems that exhibit complicated behaviors, including dissipative structures, fluctuations and oscillations, irreversible phase transitions (IPT's), etc. [1]. Partly because of their interest in real catalysis problems, in the last decades a large amount of work has been devoted to this subject, and it has been reviewed very well by Evans [2], Zhdanov and Kasemo [3], and Albano [4]. Even though it has been possible to clarify a number of phenomena observed in the laboratory, the complexity of these systems has made it difficult to check experimentally many of the theoretical advances that have been confirmed only through computer simulations.

Among the systems studied in recent years are the model proposed by Ziff, Gulari, and Barshad (ZGB) [5] for the $(A+B_2)$-type monomer-dimer reaction, which mimics the $CO+O_2$ reaction, the monomer-monomer [5,6], dimer-dimer [7], monomer-trimer [8], dimer-trimer [8,9], or the monomer-dimer-type $A+BC$ system [10–15], which mimics the reduction of NO by CO, may be mentioned. In general, in these types of systems formed by catalytic surface reactions there are two kinds of difficulties related to the characteristics of the substrate acting as a catalyst and to the knowledge of the reaction mechanism. Most of these studies, for example, assume a uniform catalytic surface that can be associated with a catalyst formed by a single crystal and a simplified kinetic mechanism for interpreting the reaction.

With respect to the first of these problems, related to the interpretation of the catalyst's surface characteristics and motivated by the fact that a large number of the catalysts are made up of tiny clusters or metal particles dispersed on an inert support, systems have been studied by modeling the catalytic surface as being part of a disordered substrate. These substrates, sometimes consisting of some kind of fractal such as, for example, percolation clusters by Albano [4,16], Casties *et al.* [17], Hovi *et al.* [18], and our group [19], diffusion-limited aggregates (DLA's) [20,21], or some deterministic fractal [22,23]. Interest in supported metal nanoparticles has been renewed recently through, for example, density functional theory (DFT) work in which the behavior of small clusters during the adsorption and oxidation of CO [24,25] has been analyzed or in temperature-programmed desorption (TPD) and infrared absorption spectroscopy (IRAS) studies of the adsorption of CO on the same kind of substrates [26].

This paper deals with the monomer-dimer-type $A+BC$ surface reaction, which mimics the reduction of NO by CO, which was studied initially by Yaldran and Khan [27], Brosilow and Ziff (BZ) [10], and Meng, Weinberg, and Evans (MWE) [11] through Monte Carlo (MC) simulations and mean-field theories (MFT's) at the site level, assuming a simplified mechanism that we will call the BZ model. This system showed an interesting surface poisoning phenomenon that was recently extended by our group to the study of disordered two- and three-dimensional substrates [21] using MC experiments. From the theoretical standpoint, our group extended the study of this reaction through MFT models at the pairs level for the BZ model [13], and for a complete kinetic mechanism [14], confirming the theoretical results with MC simulations. Later, Dickmann *et al.* [15] extended these analyses to different superficial lattices.

The MC simulations and MFT models developed in all these papers assume in general arbitrary specific rate constants for the stages of the assumed kinetic mechanism. In a recent paper [22] we developed an MC algorithm that considers a mechanism for the CO-NO reaction largely accepted at present in the experiment proposed by Permana *et al.* [28] and Peden *et al.* [29]. There we discussed the difficulty of having adequate kinetic parameters and considered a set of them reasonably representative of the experimental system for studying the behavior of this reaction on a uniform surface and on some disordered substrates, comparing qualitatively the results with some observations on the experiment.

In this paper we use the MC algorithm developed previously [22], which from the standpoint of the chosen mechanism and kinetic constants is assumed to be reasonably representative of an experimental system, to study a kind of surface that attempts to mimic a supported catalyst and is made up, as explained later, by depositing elements that rep-

*Electronic address: jcortes@dqb.uchile.cl

resent the catalytic sites on a substrate that has the characteristics of a deterministic fractal. This gives rise to a distribution of clusters similar to those seen, for example, in a typical catalyst formed by metal particles deposited on an inert support. In this way we will carry out the analysis of the CO-NO reaction on the various graphs made of trees and structures that include cycles, representative of the supported particles, allowing the study of different aspects of the system such as the catalyst's reactivity and poisoning, structural sensitivity, and others seen in the experiment.

II. MODEL AND SIMULATION

A. Reaction mechanism

The CO-NO reaction was initially studied by MC simulations and the MFT model assuming the following simplified Langmuir-Hinshelwood (LH) mechanism that we shall call BZ:

$$\mathrm{CO} + S \longrightarrow \mathrm{CO}(a),$$

$$\mathrm{NO} + 2S \xrightarrow{1} \mathrm{N}(a) + \mathrm{O}(a),$$

$$\mathrm{CO}(a) + \mathrm{O}(a) \xrightarrow{1} \mathrm{CO}_2 + 2S,$$

$$\mathrm{N}(a) + \mathrm{N}(a) \xrightarrow{1} \mathrm{N}_2 + 2S,$$

where (a) refers to the adsorbed species and S is a superficial site.

A very interesting argument given by BZ [10] and analyzed later by MWE [11] shows that the system leads inevitably to its poisoning by a process of "checkerboarding" of $\mathrm{N}(a)$ atoms if a two-dimensional and uniform square catalytic lattice is assumed. This concept was extended by our group to the case of other two- and three-dimensional disordered systems [21]. These examples show the existence of absorbent or poisoned states as a consequence of considering a simplified mechanism, a situation that is not seen in the experiment, which shows more complex mechanisms with additional stages that break up the poisoned states. Such states may appear, however, if some catalytic substrates such as those that will be seen below are considered, in spite of the assumption of complex mechanisms such as those of the experiment. Some aspects of the mechanisms discussed by the experimenters will be commented on below.

From the experimental viewpoint, the CO-NO reaction, together with the CO oxidation reaction, has been the subject of numerous studies because of its importance in pollution control in catalytic converters. Extensive reviews of the literature on these catalytic systems have been published by Taylor and by Shelef and Graham [30] and by Zhdanov and Kasemo [31]. The CO-NO reaction has been shown to be highly complex, and a series of controversies related to their mechanism and to the influence of the structural characteristics of the catalyst's surface have kept alive its present interest in the literature. A series of mechanisms have been proposed since the first papers by Hecker and Bell [32], such as those of Oh *et al.* [33], Cho [34], and Chuang and Tan [35] and those of Permana *et al.* [28] and Peden *et al.* [29], which will be used in this paper. The latter, as a result of experimental work with rhodium, proposed the LH mechanism, largely accepted at present, which considers the adsorption-desorption steps of CO and NO followed by the dissociation of NO and the surface reactions between some adsorbed species. This mechanism excludes, based on their laboratory experiments for this system, other effects such as diffusion of the adsorbed species. This model, which we shall call the Peden-Permana mechanism, has been used in the MC algorithm in this paper, and it assumes the following steps:

$$\mathrm{CO} + S \xrightarrow{k_1} \mathrm{CO}(a), \tag{1}$$

$$\mathrm{CO}(a) \xrightarrow{k_2} \mathrm{CO} + S, \tag{2}$$

$$\mathrm{NO} + S \xrightarrow{k_3} \mathrm{NO}(a), \tag{3}$$

$$\mathrm{NO}(a) \xrightarrow{k_4} \mathrm{NO} + S, \tag{4}$$

$$\mathrm{NO}(a) + S \xrightarrow{k_5} \mathrm{N}(a) + \mathrm{O}(a), \tag{5}$$

$$2\mathrm{N}(a) \xrightarrow{k_6} \mathrm{N}_2 + 2S, \tag{6}$$

$$\mathrm{CO}(a) + \mathrm{O}(a) \xrightarrow{k_7} \mathrm{CO}_2 + 2S, \tag{7}$$

$$\mathrm{NO}(a) + \mathrm{N}(a) \xrightarrow{k_8} \mathrm{N}_2\mathrm{O} + 2S. \tag{8}$$

B. Catalytic substrate

In general, supported catalysts represent an interesting example of disordered systems. Although a large amount of simulation work has been done modeling this kind of cata-

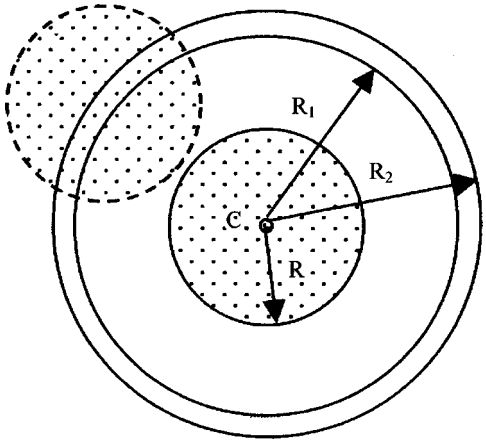

FIG. 1. Scheme of two neighbor catalytic particles of radius R deposited on fractal FRX. Details explained in the text.

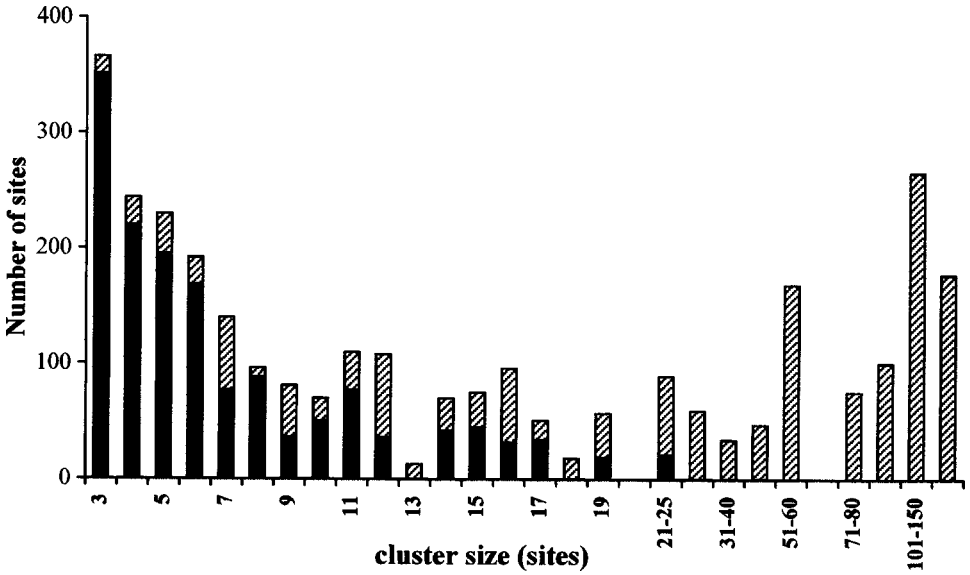

Distribution of sites (catalytic particles) according to cluster size for a substrate of 1540 elements obtained for FD=1.5 and $f_v=1.1$ ■ tree graph ▨ cyclic graphs.

lytic surface using various known fractals, as commented in the Introduction, experimental work using electron microscopy [36,37] shows that these surfaces rather consist of a series of unconnected clusters whose size distribution has been determined in catalytic studies by various experimenters [37,38]. Since the work of Avnir *et al.* [39] assumes that a solid at the nanoparticle level is a fractal, we chose a deterministic fractal, which we have previously called an FRX substrate [21,22], as the support on which we have simulated the deposition of the clusters of catalytic particles.

The catalytic substrate was then built by first generating 30 000 points of the support belonging to the FRX fractal as described in the Appendix, using 21 transformations, leading to a fractal dimension equal to 2.771 [40,41]. In fractal FRX, if d is the average distance between a site and its nearest neighbor, all the sites within a sphere of radius $2d$ centered at the site were considered neighbors of a given site. This gave rise to a rather unrealistic situation in which some sites have a large number of neighbors, e.g., of the order of 20—30 sites, and others have very few or even none. In our model's substrate it is assumed that each supported element is a sphere of radius R with its center at some point of fractal FRX. That element may represent a supported metal atom; one can imagine a rhodium atom, for example, a typical active site in the catalysts used in the case of the CO-NO reaction.

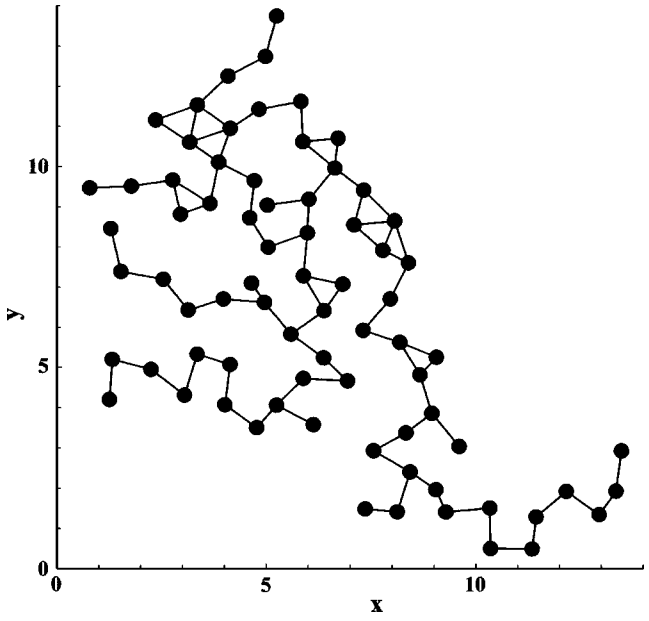

FIG. 3. Cluster of 75 substrate sites corresponding to Fig. 2. x,y (particle diameter).

The supported substrate is generated as follows: Any point is chosen on fractal FRX as the center of a first element of radius R, and then all the points on the fractal located within a sphere of radius $2R$ are discarded from the list of possible centers. The point of FRX closest to the first element is chosen as the center of the second element, and once again all the points located within a sphere of radius $2R$ centered on that point are discarded. The third element chosen will now be the one closest to the second one, and this is done repetitively until there are no points on the support with sufficient space to locate a new element. The radius R of the element is defined as a function of the distance d according to $R=\mathrm{FD}\times d$, where factor FD, which we have called the diameter factor, is varied with the purpose of changing the cluster distribution obtained.

At the end of this process a set of catalytically active sites of radius R is obtained whose centers are located in a fractal. If the maximum distance allowed between the sites for them to be considered neighbors is defined adequately, the sites of the catalyst's set are grouped in clusters, with each cluster containing those sites that have a neighborhood relation between them. For example, within a hard-sphere scheme we can consider as neighbors in our substrate two sites whose centers are at a distance $R_1=2R$. In this paper, however, we have given some breadth to the system and have assumed that two sites are nearest neighbors (NN) if their centers are at a distance between $R_1=2R$ and $R_2=2Rf_v$, where f_v is a neighborhood factor, with $f_v>1$. Figure 1 shows a site of the substrate whose center is at point C of the support and a neighboring site whose center is within the spherical hull

TABLE I. Kinetics constants of the Peden-Permana mechanism at two temperatures. k_i (s^{-1}), P_i (torr), and $P_{CO}+P_{NO}=16$ (torr).

$T(K)$	k_1	k_2	k_3	k_4	k_5	k_6	k_7	k_8
623	$82804p_{CO}$	1.56×10^4	$80003P_{NO}$	1.75×10^4	1.21×10^4	14.6	9.62×10^6	178.7
800	$73072P_{CO}$	2.56×10^6	$70600P_{NO}$	3.54×10^6	2.91×10^5	4959	1.24×10^8	61704

located between distances R_1 and R_2 from center C as seen in the figure.

The elements of a cluster can be joined by lines to their respective next neighbors. In mathematical terminology these clusters are graphs that may be cyclic if they include at least one closed circuit; otherwise, they are trees. Figure 2 shows a distribution of the number of sites of the substrate, according to cluster size, obtained by this method for FD $=1.5$ and $f_v=1.1$, where the sites belonging to clusters having at least one cycle are shown separately from those belonging to graphs that are trees. In this case a support was generated with 30 000 initial points, giving a total of 1540 sites. It should be noted that no trees are found corresponding to clusters greater than about 25 sites. Figure 3, on the other hand, shows a substrate cluster with 75 elements that has 11 cycles joined by branched structures of various shapes. It should be kept in mind that the figure shows some spatial deformation because the points of support FRX are distributed in three dimensions, albeit with a small thickness in the z direction.

C. Reaction simulation procedure

The MC algorithm used in this paper is similar to one used previously by our group [42] for the CO oxidation reaction, based on one proposed earlier for this system [43] and recently by us [22] and Olsson, Zhadanov, and Kasemo [44] for the CO-NO reaction. For the previous reaction the simulation process began by selecting an event from the mechanism (1)–(8) (adsorption, desorption, dissociation, or reaction) according to the probability p_i of the occurrence of the event defined by

$$p_i = k_i \Big/ \sum_i k_i, \tag{9}$$

where k_i corresponds to the rate constant of step i of the mechanism (1)–(8). It is assumed that the rate constants k_i can be expressed as functions of temperature T according to Arrhenius' equation

$$k_i = \nu_i \exp(-E_i/RT), \tag{10}$$

where E_i is the activation energy and ν_i is the frequency factor. An exception is made in the case of adsorption, in which k_i was calculated according to the kinetic theory of gases expression

$$k_j(\text{ads}) = S_j\sigma(2\pi M_j RT)^{-1/2}P_j \quad (j=\text{CO,NO}), \tag{11}$$

where M_j is the molecular mass of j, S_j is the corresponding sticking coefficient ($S_{CO}=S_{NO}=0.5$), the coefficient σ is the area occupied by 1 mol of superficial metal atoms [3.75×10^8 cm^2/mol for Rh(111)] [33], and P_j is the pressure of element j in the gas phase.

The MC algorithm begins with the selection of the event. If it corresponds to the adsorption of CO, a site is chosen randomly on the surface, and if it is vacant, a CO(a) particle will be adsorbed. If the site is occupied, the attempt is ended. If the adsorption of NO is chosen, the procedure is completely analogous and a NO(a) particle is adsorbed.

If CO desorption is chosen, a surface site is selected randomly. If it is occupied by a particle different from CO(a) or it is vacant, the attempt is ended. However, if it is occupied by a CO(a) particle, desorption occurs and the particle is replaced by a vacant site. The procedure is analogous in the case of choosing the desorption of NO.

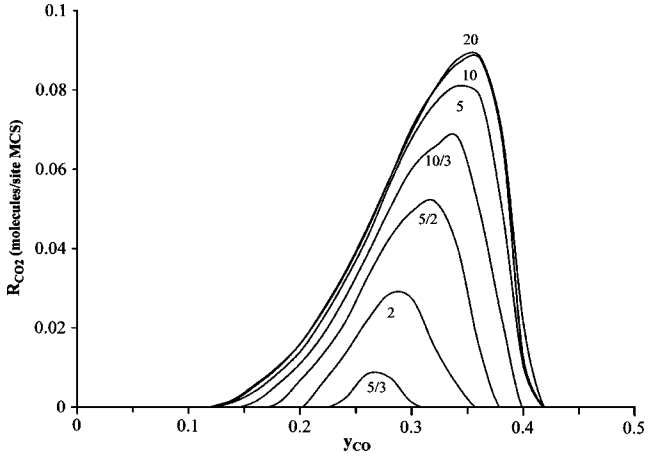

FIG. 4. Production of CO_2 (R_{CO_2}) versus CO concentration in the gas phase for the BZ mechanism of the CO-NO reaction for different values of f_v (FD$\times$ $f_v=1$).

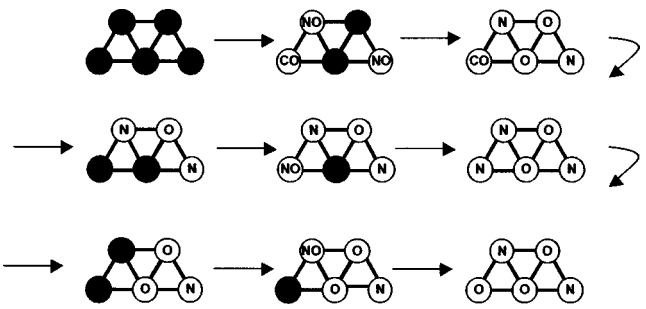

FIG. 5. One possible poisoning sequence for a cyclic cluster of five sites.

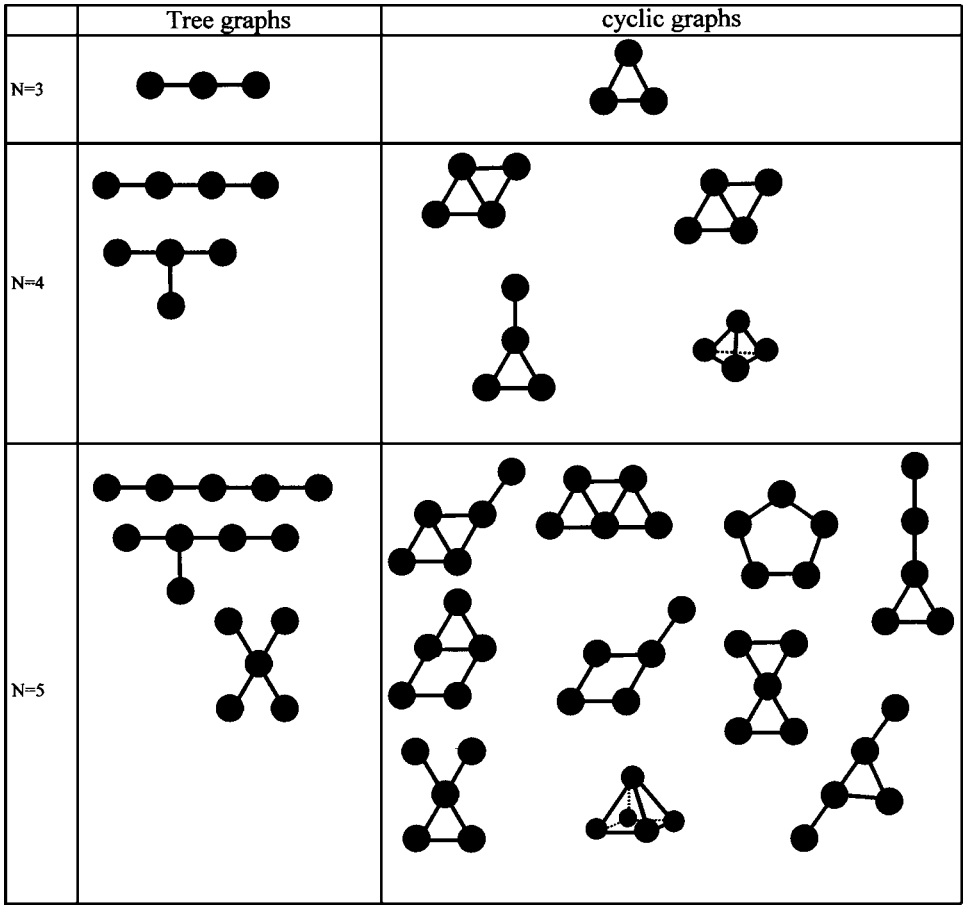

FIG. 6. Tree type and cyclic graphs for clusters of $N=3$–5 sites.

In the case of chemical reaction events, a site on the surface is first chosen randomly. If it is occupied by a particle corresponding to the selected reaction, an NN site is then chosen randomly next to the first site. If the latter is occupied by the other particle necessary for the reaction, the event is successful and a product molecule is removed from the surface, leaving two vacant sites. For example, if the first particle is CO(a) and the second is O(a), a molecule of CO_2 leaves the surface.

When the chosen event is the dissociation of NO, a surface site is chosen randomly. If it is occupied by a NO(a) particle, an NN site is chosen randomly next to the first site. If this is empty, dissociation occurs and a N(a) particle remains in the first site and an O(a) particle in the second site. However, if the first site was originally empty and the second NN site is occupied by a NO(a) particle, dissociation occurs and an O(a) particle remains in the first site and a N(a) particle in the second site.

The MC experiments were carried out over the substrate described in the previous section assuming that a catalytic site is the element of radius R supported on the FRX fractal. The dynamics of the process was studied as a function of Monte Carlo steps (MCS), defined as a number of attempts equal to the number of sites in the substrate. Production, however, expressed as turnover number (TON), the number of molecules of the product per site and per second, was obtained by carrying out the transformation in real time.

III. RESULTS AND DISCUSSION

A. Comparison of the model with the mathematical limit FRX

When the BZ model is applied to the substrate constructed in this paper, a rapid poisoning of the surface occurs, the same as for a square lattice, although in previous work on the FRX fractal (which is actually the support) a reactive window had been obtained [40,41]. With the purpose of studying this difference, we have changed gradually the substrate from the extreme case where the catalyst would be a mathematical substrate, the FRX fractal, in which the site is a point and has an extensive spherical neighborhood hull, to substrates in which the site is no longer a point but a sphere of radius R, while the extension allowed for the neighborhood hull gets smaller. To make the previous comparison we have varied artificially the diameter factor FD, keeping $R_2=2d$ constant and setting the value of the product $\mathrm{FD}\times f_V=1$. The extreme situation, when $\mathrm{FD}\rightarrow 0$, corresponds to the mathematical FRX fractal, whose elements can have up to 30 neighbors, thereby preventing the poisoning over a wide range of y_{CO}, the concentration of CO in the gas phase. As FD increases, f_V decreases, so the number of neighbors per element decreases until the other extreme, when $\mathrm{FD}\rightarrow 1$, is reached, with $R_1=R_2$, which in this hypothetical example would mean that there are only isolated sites and consequently production is nil.

Figure 4 shows the above situation in which it is seen that production is greater the greater the neighborhood factor,

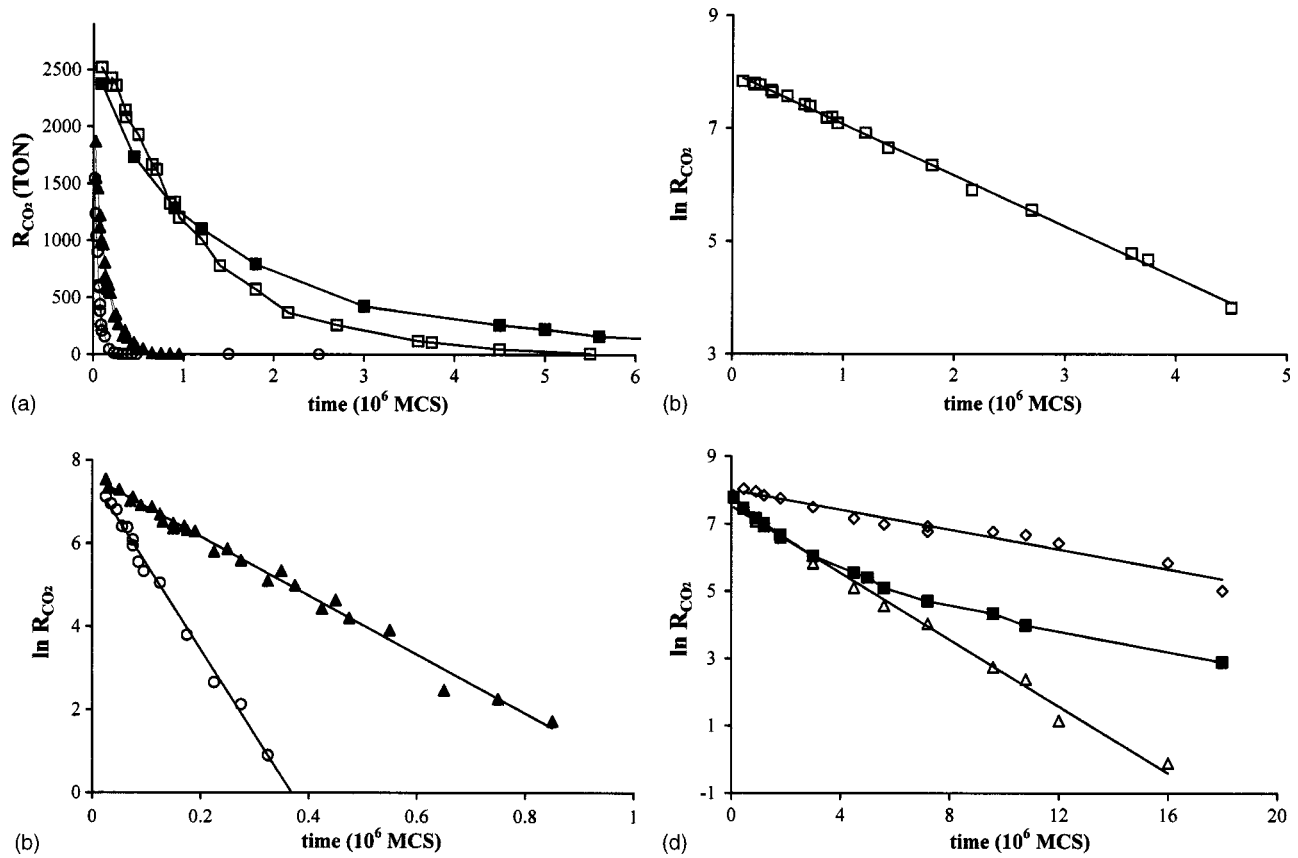

FIG. 7. Evolution of production over time for clusters of three and five sites. (a) R_{CO_2} vs time: ○ trees of three sites ▲ trees of five sites □ cyclic graphs of three sites ■ cyclic graphs of five sites. (b) ln R_{CO_2}vs time ○ trees of three sites ▲ trees of five sites. (c) ln R_{CO_2}vs time cyclic graphs of three sites. (d) ln R_{CO_2}vs time; for cyclic clusters of five elements; △ clusters of one cycle. ◇ Cluster ⩾ two cycles; ■ all the cyclic clusters.

since high values of f_v lead to large numbers of neighbors, together with a large number of cycles, thereby increasing the system's productivity. The reactive window, on the other hand, decreases together with production toward smaller f_v values and, finally, closes for neighborhood factors lower than approximately 1.4, causing poisoning of the catalytic substrate.

B. Productivity and poisoning

In what follows we will consider the Peden-Permana mechanism given by reactions (1)–(8). We have also chosen the set of rate constants shown in Table I corresponding to activation energies and frequency factors proposed by Oh *et al.* [33] and Belton *et al.* [45] for the CO-NO reaction over rhodium obtained from experimental data. This makes it possible to study qualitatively the behavior of our systems, in spite of the rather abstract model chosen for the catalytic surface, approaching more closely the experimental results than an approach using arbitrary rate constants, such as that of most of the simulation work found in the literature.

The first aspect of interest to us, which corresponds to the results shown in the figures that follow, is related to the possibility that some clusters in the substrate are poisoned during the kinetic process and later do not take part in the reaction. Another aspect considers the laws that govern the evolution in time of those processes, regardless of whether they lead to poisoning of the surface. There is no doubt that these situations have practical importance. On the other hand, they are matters of theoretical interest in the dynamics of irreversible processes. Figure 5 is an illustration of a sequence, among others that are possible, of the CO-NO reaction that occurs on a cluster of five catalytic sites, leading to an absorbent or poisoned configuration of the cluster.

In order to follow the dynamics of these kinds of processes we have graphed the evolution in time of the production of CO_2 for sets of clusters generated with $F_D=1.5$ and $f_v=1.1$, separating them by size and/or kind. Figure 6 shows all the possible cyclic graphs and trees of clusters having between three and five sites, and Fig. 7 shows the evolution in the case of clusters of three and five sites at 800 K and equal CO and NO pressure of 8 Torr in the gas phase. Figure 7(a) shows production versus simulation time in clusters of three and five sites, separating the cases of trees and cyclic clusters. Figure 7(b), on the other hand, shows the logarithm of production against time under the same conditions in the case of trees of three and five elements. It is interesting to see the good linearity achieved, showing that CO_2 production decreases with time in these cases according to an empirical law of the following kind:

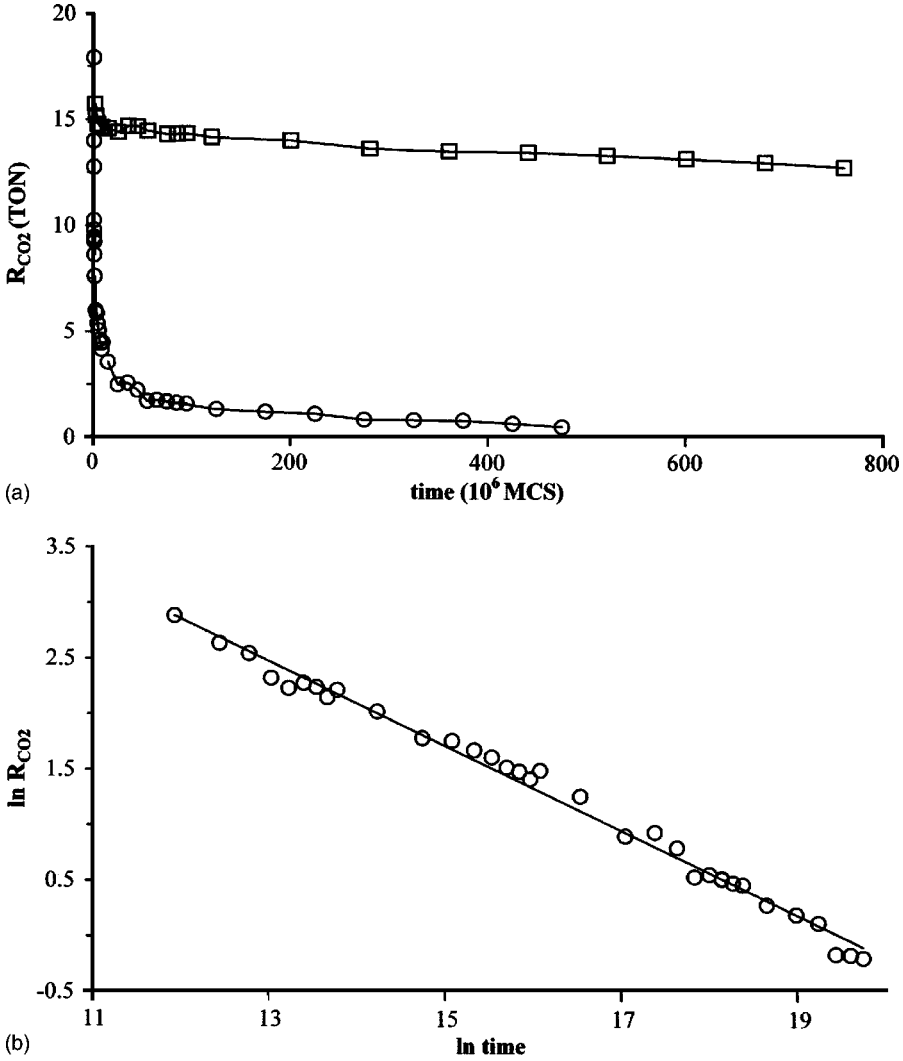

FIG. 8. Evolution in time of production of all substrate's clusters. (a) R_{CO_2} vs time ○ trees; □ cyclic graphs (b) $\ln R_{CO_2}$ vs in time for all the substrate's tree type clusters.

$$\ln R_i = -kt + b, \tag{12}$$

where k and b are constants. The same situation was reached in the cyclic clusters of three sites, as seen in Fig. 7(c). On the other hand, Fig. 7(d) shows an interesting situation corresponding to clusters of five sites. The above linearity is fulfilled separately in clusters of five sites that have only one cycle or two or more cycles. However, the linearity is lost if the substrate formed by all the cyclic clusters of five elements is considered, since in that case the one-cycle clusters are poisoned more rapidly, so at the beginning the curve follows their trend and at the end the trend of the remaining ones. In all cases in which relation (12) was followed, a linear relation was also obtained between production and the number of clusters that remain active. This shows that the decay of production with time is caused by the disappearance of the clusters that are no longer active due to poisoning.

Figure 8(a) shows separately for trees and cyclic graphs the evolution in time of production in the case of substrates composed of all the clusters of the substrate. When considering clusters of all sizes, no linearity like that of Eq. (12) is seen, since the smaller clusters are poisoned first and stop contributing to production. Linearity was seen, however, for $\ln R_{CO_2}$ versus $\ln t$ in the case of all the trees, as shown in Fig. 8(b), corresponding in that case to a scaling law of type

$$R_i = At^m, \tag{13}$$

where A and m are constants. It is interesting to see that in the cases studied the set of trees is poisoned, while for the set of cyclic graphs production tends to become stabilized and no poisoning is observed for such long times as 800×10^6 MCS. It was also seen that production remains stable in a cluster of 75 sites, with no poisoning occurring at times as long as $12\,000 \times 10^6$ MCS. This allows us to state that the system of large clusters reaches a pseudo steady state which is sufficient to consider stationary the results of the phase diagrams that will be seen later, and it also explains what is found in experimental practice.

The constants in expressions (12) and (13) are parameters that depend on temperature because they are functions of the rate constants. The processes become slower as the temperature decreases, making it difficult to observe the simulation of the phenomenon at lower temperatures.

Figure 10 shows poisoning time versus the number of cycles for a sequence of honeycomb-type clusters shown in Fig. 9, which we have defined as the time needed for poison-

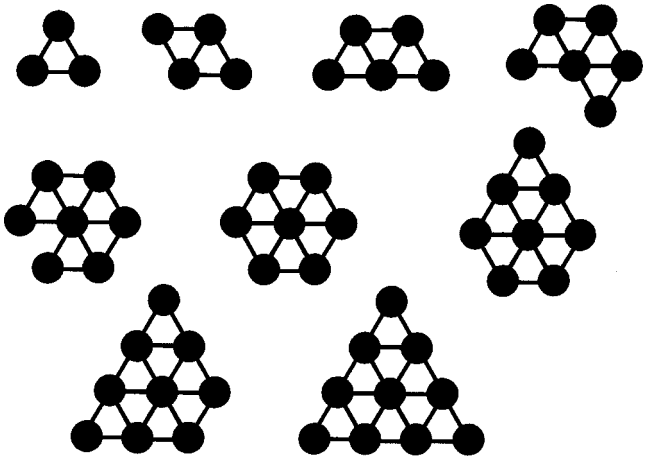

FIG. 9. Honeycomb-type cluster sequence corresponding to Fig. 10.

ing a fraction of the clusters if the CO-NO reaction process is carried out on a substrate formed by 25–100 identical clusters. What we find interesting in this figure is the rising increment seen when the number of cycles is increased. We have confirmed this effect by computer experiments carrying out the process on a single cluster of N cycles. Although certainly with a greater dispersion, the behavior was qualitatively the same as that of Fig. 10.

C. Phase diagrams

The above results allow us to assume that it is possible to obtain phase diagrams for which a reasonable steady state has been achieved. Figure 11 shows the production and coverage of the different superficial species versus gas phase concentration at 800 K, and in the insets we have also graphed the production and coverage at 623 K.

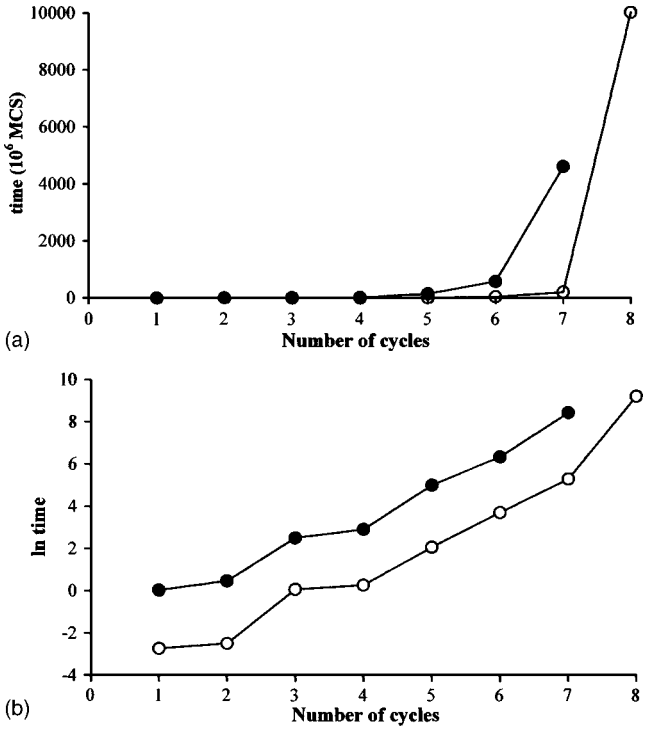

FIG. 10. Poisoning time needed to poison 4% (○) and 50% (●) of the clusters vs number of cycles for the honeycomb type substrates of Fig. 9.

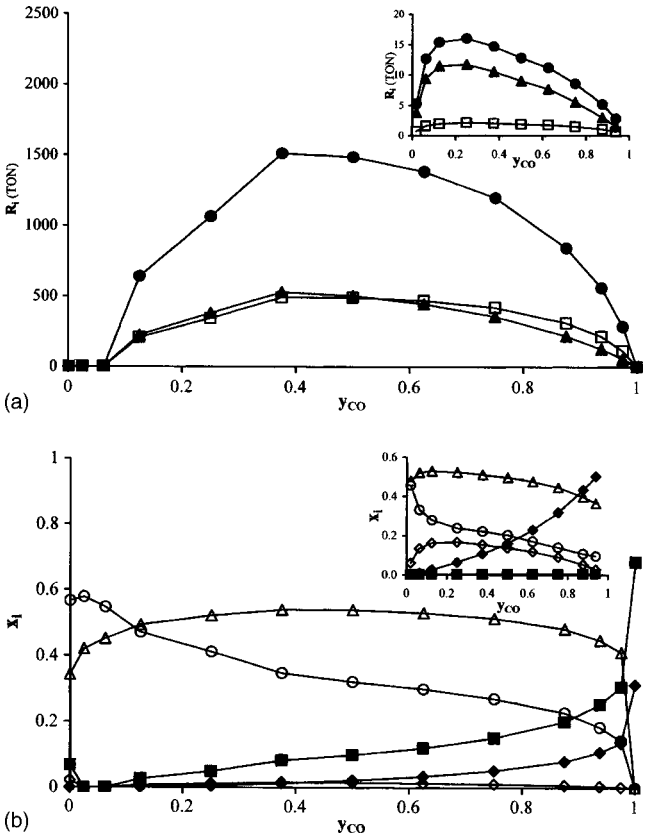

FIG. 11. Production and phase diagrams versus CO concentration in the gas phase for the Peden-Permana mechanism of the CO-NO reaction at 800 K, $P_{CO}+P_{NO}=16$(torr). (The insets show the corresponding cases for 623 K.) (a) R_{CO_2} (●), R_{N_2} (□), R_{N_2O} (▲) and (b) x_{CO} (♦), x_{NO} (◇), x_O (○), x_S (■), x_N (△).

In general it is not possible to ensure the existence of phase transitions such as those of the classical ZGB model [5] from the results reported in the paper. As to the experimental data, Fig. 11(a) shows an interesting agreement between the magnitude of production and the literature reports for the CO-NO reaction over rhodium—for example, at 623 K in the work of Oh *et al.* [33]. The results are smaller than those obtained on homogeneous surfaces which, as is well known, are always greater than on supported surfaces, as seen in the data reported by Oh *et al.* [33] for the system.

It is also seen that production is largely dependent on temperature. At 623 K production is rather negligible compared to that at 800 K. This is accounted for by the important dependence of some reaction constants on temperature, as can be seen in Table I. For example, at 623 K the adsorption constants are greater than the desorption constants, producing few empty sites and thereby hindering the dynamics of the reaction and leading to a quasipoisoned surface with very small production. This situation contrasts with the process at 800 K, for which the table shows that desorption is high compared to adsorption, producing a significant fraction of vacant sites at CO concentrations, y_{CO}, higher than 0.06. This situation, together with the additional increase in the reaction

and dissociation constants, leads to high system reactivity, with production about 100 times greater than at 623 K.

The relative magnitudes of the reaction constants in Table I also explain other particulars of the phase and production diagrams of Fig. 11. For example, dissociation is greater at 800 K than at 623 K because at 800 K there is a greater proportion of empty sites and a higher dissociation constant. This accounts for the small amount of NO on the surface at 800 K and its relative accumulations at 623 K. Superficial nitrogen is high in both cases because of the low value of the constant of reaction (6), while superficial oxygen is lower at 800 K because it is consumed by reaction (7) whose rate constant is high, and this also results in a greater production of CO_2. At 623 K production of N_2O is greater than that of N_2 due to the relative differences between the reaction rate constants. However, at 800 K both productions are approximately equal because of the relative decrease in NO converge on the surface.

In the CO concentration range below 0.06% at 800 K there is no production, and the surface is essentially poisoned with superficial oxygen and nitrogen. In these systems without diffusions, superficial mobility occurs through the successive and rapid desorption of CO and NO and their corresponding reactions. If the fraction of vacant sites is negligible, all the processes become very slow and the system tends to become poisoned as in this case, in which the oxygen is not removed through reaction (7) because of the low amount of CO adsorbed in this region. Also, the N(a) is not removed by reaction (8) because there is no superficial NO. At 623 K poisoning with oxygen is less, leading to a larger amount of nitrogen which together with the existence of a small amount of NO, accounts for the existence of production, albeit small, in the system.

ACKNOWLEDGMENT

The authors thank FONDECYT Grant No. 1030759 for financial support of this work.

APPENDIX

The FRX substrates were obtained by generating a series of deterministic fractals of different dimensions based on a symmetry-theoretical concept of fractal geometry [46] in the same way as the surfaces used by Park *et al.* [40,41] in MC studies of catalytic CO oxidation. The method consists of the construction of multifractal surfaces by the repetition of self-similar structures within a structure at successively finer length scales, assigning a set of affine transformations $\{\omega_i\}$ which contract and move the structure, such that the union of these images constitutes the given fractal itself: i.e.,

$$X = \bigcup_{i=1}^{n} \omega_i(X), \tag{A1}$$

where X is the fractal and n is the number of associated affine transformations [46]. If λ_i is the scaling factor of the ith affine transformation, ω_i, it is possible to determine the dimension D of the fractal from the relation

$$\sum_{i=1}^{n} \lambda_i^D = 1. \tag{A2}$$

In our work we consider a fractal support defined by sets of affine transformations of the form

$$\omega_i \begin{pmatrix} x \\ y \\ x \end{pmatrix} = \lambda_i \begin{pmatrix} \cos\theta_i & -\sin\theta_i & 0 \\ \sin\theta_i & \cos\theta_i & 0 \\ 0 & 0 & 1 \end{pmatrix} \begin{pmatrix} x \\ y \\ z \end{pmatrix} + \begin{pmatrix} l_i \\ m_i \\ n_i \end{pmatrix}, \tag{A3}$$

considering the scaling factor λ_i equal to $1/3$ in all of them. The values of the rotational angles θ_i and the translations l_i, m_i, and n_i in the respective x, y, and z directions are those given in Table I of Ref. [40]. In general, fractals of different dimension can be obtained by changing the number of affine transformations and the associated scaling factors.

To construct the fractals on the computer, use was made of the random iteration algorithm [40,41] as follows: a sequence of spatial points $\{\mathbf{r}_N: N=0,1,2,\ldots\}$ is generated recursively by applying the transformation

$$\mathbf{r}_N = \omega_i(\mathbf{r}_{N-1}) \tag{A4}$$

from any point $\mathbf{r}_0$ in space—e.g., the origin. At each step, a particular transformation—say, ω_i—is selected with an assigned probability p_i from an arbitrary set $\{p_i\}$ such that $\Sigma_1 p_i = 1$. In our case 30 000 points were generated in this way, becoming the active sites of the FRX substrates. Neighbors of a site of the FRX fractal are considered to be all those fractal sites located in a spherical environment of radius $2d$, defined, following Park *et al.* [40,41], as twice the average distance between every surface site and its nearest neighbor.

[1] G. Nicolis and I. Prigogine, *Self-Organization in Nonequilibrium Systems* (Wiley Interscience, New York, 1977); H. Haken, *Synergetics* (Springer-Verlag, New York, 1977); J. Marro and R. Dickman, *Nonequilibrium Phase Transitions in Lattice Models* (Cambridge University Press, Cambridge, England, 1999).
[2] J. W. Evans, Langmuir **7**, 2514 (1991).
[3] V. P. Zhadanov and B. Kasemo, Surf. Sci. Rep. **20**, 111 (1994).
[4] E. V. Albano, Heterog. Chem. Rev. **3**, 389 (1996); E. V. Albano and M. Borówko, *Computational Methods in Surface and Colloid Science* (Marcel Dekker, New York, 2000), Chap. 8, pp. 387–437.
[5] R. M. Ziff, E. Gulari, and Y. Barshad, Phys. Rev. Lett. **56**, 2553 (1986).
[6] K. Fichthorn, E. Gulari, and R. Ziff, Phys. Rev. Lett. **63**, 1527 (1989); Chem. Eng. Sci. **44**, 1403 (1989); E. Albano, Phys. Rev. A **46**, 5020 (1992).
[7] K. M. Khan, K. Yaldram, and N. Ahmad, J. Chem. Phys. **109**, 5054 (1998).
[8] K. M. Khan, K. Yaldram, N. Ahmad, and Qamar-ul-Haque,

Physica A **268**, 89 (1999); K. M. Khan, A. Basit, and K. Yaldram, J. Phys. A **33**, L215 (2000).
[9] D. ben-Avraham and J. Kohler, J. Stat. Phys. **65**, 839 (1991).
[10] B. J. Brosilow and R. M. Ziff, J. Catal. **136**, 275 (1992).
[11] B. Meng, W. H. Weinberg, and J. W. Evans, Phys. Rev. E **48**, 3577 (1993).
[12] K. Yaldram and M. A. Khan, J. Catal. **131**, 369 (1991).
[13] J. Cortés, H. Puschmann, and E. Valencia, J. Chem. Phys. **105**, 6026 (1996).
[14] J. Cortés, H. Puschmann, and E. Valencia, J. Chem. Phys. **109**, 6086 (1998).
[15] A. Dickman, B. C. Grandi, W. Figueiredo, and R. Dickman, Phys. Rev. E **59**, 6361 (1999).
[16] E. V. Albano, Phys. Rev. B **42**, 10818 (1990); Surf. Sci. **235**, 351 (1990); Phys. Rev. A **46**, 5020 (1992).
[17] A. Casties, J. Mai, and W. von Niessen, J. Chem. Phys. **99**, 3082 (1993).
[18] J. P. Hovi, J. Vaari, H. P. Kaukonen, and R. M. Nieminen, Comput. Mater. Sci. **1**, 33 (1992).
[19] E. Valencia and J. Cortés, Surf. Sci. **470**, L109 (2000); J. Cortés and E. Valencia, Physica A **309**, 26 (2002).
[20] J. Mai, A. Casties, and W. von Niessen, Chem. Phys. Lett. **211**, 197 (1993).
[21] J. Cortés and E. Valencia, Phys. Rev. E **68**, 016111 (2003).
[22] J. Cortés and E. Valencia, J. Phys. Chem. B **108**, 2979 (2004).
[23] J. Mai, A. Casties, and W. von Niessen, Chem. Phys. Lett. **196**, 358 (1992); A. Tretyakov and H. Takayasu, Phys. Rev. A **44**, 8388 (1991); Zhuo Gao and R. Yang, Phys. Rev. E **60**, 2741 (1999); I. Jensen, J. Phys. A **24**, L111 (1991).
[24] D. W. Yuan and Z. J. Zeng, Chem. Phys. **120**, 6574 (2004).
[25] L. M. Molina, M. D. Rasmussen, and B. Hammer, J. Chem. Phys. **120**, 7673 (2004).
[26] C. Lemire, R. Meyer, Sh. K. Shaikhutdinov, and H. J. Freund, Surf. Sci. **552**, 27 (2004).
[27] K. Yaldram and M. A. Khan, J. Catal. **131**, 369 (1991).
[28] H. Permana, K. Simon Ng, Ch. Peden, S. J. Schmieg, D. K. Lambert, and D. Belton, J. Catal. **164**, 194 (1996).
[29] Ch. Peden, D. Belton, and S. J. Schmieg, J. Catal. **155**, 204 (1995).
[30] K. C. Taylor, Catal. Rev. Sci. Eng. **35**, 457 (1993); M. Shelef and G. Graham, *ibid.* **36**, 433 (1994).
[31] V. P. Zhdanov and B. Kasemo, Surf. Sci. Rep. **29**, 31 (1997).
[32] W. C. Hecker and A. T. Bell, J. Catal. **84**, 200 (1983).
[33] S. H. Oh, G. B. Fisher, J. E. Carpenter, and D. Wayne, J. Catal. **100**, 360 (1986).
[34] B. K. Cho, J. Catal. **138**, 255 (1992); **148**, 697 (1994).
[35] S. Chuang and C. Tan, J. Catal. **173**, 95 (1998).
[36] Ch. Wong and R. W. McCabe, J. Catal. **107**, 535 (1987); S. Chakraborti, A. K. Datye, and N. J. Long, *ibid.* **108**, 444 (1987).
[37] D. R. Rainer, S. M. Vesecky, M. Koranne, W. S. Oh, and D. W. Goodman, J. Catal. **167**, 234 (1997).
[38] S. H. Oh and C. C. Eickel, J. Catal. **128**, 526 (1991); A. G. Sault and V. Tikare, *ibid.* **211**, 19 (2002); G. Prevot, O. Meerson, L. Piccolo, and C. R. Henry, J. Phys.: Condens. Matter **14**, 4251 (2002).
[39] D. Avnir, D. Farin, and P. Pfeifer, Nature (London) **308**, 261 (1984); P. Pfeifer and D. Avnir, J. Chem. Phys. **79**, 3558 (1983); D. Avnir, D. Farin, and P. Pfeifer, *ibid.* **79**, 3566 (1983).
[40] H. Park H. Kim, and S. Lee, Surf. Sci. **380**, 514 (1997).
[41] H. Park and S. Lee, Surf. Sci. **411**, 1 (1998).
[42] J. Cortés, E. Valencia, and P. Araya, J. Chem. Phys. **109**, 5607 (1998).
[43] P. Araya, W. Porod, and E. Wolf, Surf. Sci. **230**, 245 (1990); P. Araya, W. Porod, R. Sant, and E. Wolf, *ibid.* **L80**, 208 (1998).
[44] L. Olsson, V. P. Zhdanov, and B. Kasemo, Surf. Sci. **529**, 338 (2003).
[45] D. N. Belton, C. L. DiMaggio, S. J. Schmieg, and K. Y. Simon Ng, J. Catal. **157**, 559 (1995).
[46] M. F. Barnsley, *Fractals Everywhere* (Academic Press, New York, 1988); in *Proceedings of the Symposia in Applied Mathematics*, edited by R. L. Devaney and L. Keen (American Mathematical Society, Providence, RI, 1988), Vol. 39.